# P4.7 Investigation of a severe downburst storm near Phoenix, Arizona as seen by a mobile Doppler radar and the KIWA WSR-88D

Steven Vasiloff and Kenneth Howard
National Severe Storms Laboratory, Norman, OK

## 1. INTRODUCTION

During the past ten years, the frequency of damaging winds from downbursts occurring in the Phoenix metropolitan area and surrounding suburbs has markedly increased presumedly due to population growth and better reporting (SPC 2007). Within the Southwestern United State's Sonoran Desert, downbursts frequently produce strong outflows that entrain dust and reduce visibility to dangerous levels, particularly hazardous to traffic along the Interstate highway system in southern Arizona. Referenced locally as "haboobs," (e.g., Fig. 1) these dust storms are most frequent between May and September. These events also pose a threat to aviation and disrupt electrical service by downing overhead electrical transmission lines.

The severity of the damage to electrical power transmission lines from an engineering perspective has resulted in speculation of an especially violent class of downbursts which result in velocities and shear exceeding what has been typically observed or documented in the formal literature. In an effort to better understand and document the occurrence of Sonoran downbursts, their background environments, their severity and impacts on electrical power transmission infrastructure, the National Severe Storms Laboratory deployed a Shared Mobile Atmospheric Research and Teaching Radar (SMART-R1 (SR1); (Biggerstaff et al. 2005) in the Phoenix (PHX), Arizona during the summer of 2004. On 27-28 July, a series of severe downbursts occurred south of PHX and were observed at close range by the SR1 and the National Weather Service (NWS) KIWA Weather Surveillance Radar – 1988 Doppler (WSR-88D) radar. [Figure 2 shows a photograph taken during the time of peak surface winds associated with one of the downbursts].

Corresponding author address: Steven Vasiloff, NSSL, 120 David Boren Blvd., Norman, OK 73072; email: steven.vasiloff@noaa.gov

The observations facilitate a unique examination of the scales of motion and lifecycle structure of a series of severe downburst pulses as observed by two radars having different spatial and temporal resolutions as well as viewing perspectives. The following sections provide scientific and observational background on downbursts to ascertain whether downbursts occurring within the Sonoran Desert environment exhibit dissimilar characteristics compared to the rest of the U.S. and constitute a more extreme class or hybrid storm.

## 2. DOWNBURST BACKGROUND

Severe winds from convective storms often begin as downbursts. Fujita (1981) defined a downburst as "a strong downdraft which induces an outburst of damaging winds on or near the ground," and a microburst as "a small downburst with…damaging winds extending only 4 km (2.5 mi) or less". The Joint Airport Weather Studies (JAWS) field project in Colorado (e.g., Wilson et al. 1984; Hjelmfelt 1988) was designed to study microbursts and the associated wind shear that can be very dangerous to aircraft arriving and departing from an airport. During JAWS, observed microbursts had a median velocity difference ($\Delta v$) of 22 m $s^{-1}$ across an average distance of 3.1 km, with the median time of 5-10 min to

Figure 1. Photograph of the SR1 with a haboob in the background. Courtesy of Kenneth Howard.

Figure 2. Photograph looking SW toward the microburst dust cloud just before 0200 UTC on 28 July 2004. Courtesy of Steve Sipple with the Phoenix WFO.

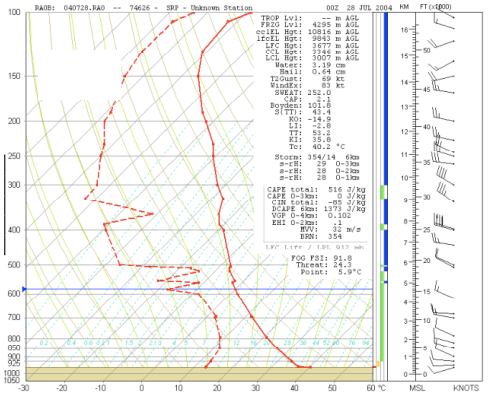

Figure 3. Sounding taken from the PHX WFO at 0000 UTC 28 July 2004.

reach the maximum Δv. Most occurred with isolated pulse storms though some occurred in conjunction with multicellular convective lines. The typical local thermodynamic environment for JAWS microbursts is characterized by a deep dry well-mixed boundary layer capped by a layer of high relative humidity (RH) with low convective available potential energy (CAPE). This environment supports the development of low-reflectivity microbursts (LRMs) where very little rain reaches the surface and strong winds are driven primarily by evaporative cooling as small raindrops and graupel fall from a relatively high cloud base into dry sub-cloud air. At the other end of the microburst spectrum high-reflectivity microbursts (HRMs) have frequently been observed in more moist environments, occur in conjunction with heavy rainfall, and are the result of evaporating rain, melting hail and precipitation loading (e.g., Atkins and Wakimoto 1991; Caracena and Meier 1987). HRMs in Florida, as described in Rinehart et al. (1995), had surface wind characteristics similar to those of JAWS microbursts. Downbursts and microbursts have also been documented in other parts of the country including Oklahoma (Eilts and Doviak, 1987) and Utah (Mielke and Carle, 1987).

## 3. STORM ENVIRONMENT ON 27 JULY 2004

Special soundings were taken from the NWS Forecast Office in PHX on 27-28 July 2004. The 2100 UTC 27 July sounding (not shown) indicated 700 – 500 mb steering winds were west-northwesterly with southwesterly surface winds. Moderate CAPE (767 J $Kg^{-1}$) was present with a 500 mb lifted index of –2.5 C. The boundary layer was well mixed with a dry-adiabatic lapse rate from just above the surface to ~720 mb and a small amount of convective inhibition (CI). Three hours later (Fig. 3), subsidence appears to have occurred in the lower troposphere; warming and a decrease in RH was observed between 700 and 800 mb was thus increasing the CI. These soundings deviate from typical LRM soundings that approach 100% RH near the top of the boundary layer. Furthermore, they were not typical Arizona microburst soundings as this was more of a transitional event with the 500 mb ridge well south of PHX with a break in the monsoon imminent (Doug Green, personal communication).

## 4. RADAR DATA ANALYSIS

The representativeness of radar observations depends primarily on the radar beam resolution volume size with respect to the ambient vertical wind shear. Sharp vertical gradients of winds as well as peak wind speeds will be smoothed

Table 1. Characteristics of the SR1 and KIWA radars.

| Attribute | SR1 | KIWA |
|---|---|---|
| Wavelength | 5 cm | 10 cm |
| Azimuthal resolution | 1 deg | 0.95 deg |
| Radial resolution | 70 m reflectivity and velocity | 1 km reflectivity; 250 m velocity |
| VCP angles | 0.5, 0.8, 1.2, 1.6, 2.1, 2.6 3.4, 4.2, 5.1, 5.9, 6.9, 7.9, 9.1, 10.2, 11.4, 12.9, 14.5, 16.3, 18.5, 20.0, 22.0, 25.0 | VCP 11: 0.5, 1.45, 2.4, 3.35, 4.3, 5.25, 6.2, 7.5, 8.7, 10.0, 12.0, 14.0, 16.7, 19.5 |
| VCP intervals | 3-5 min | 5 min |

out/diminished if they occur over a small distance compared to a radar beam volume dimensions. For example, Eilts (1987) used instrumented tower data to show that radar under-estimated vertical shear in gust fronts while over-estimating surface winds. Vasiloff

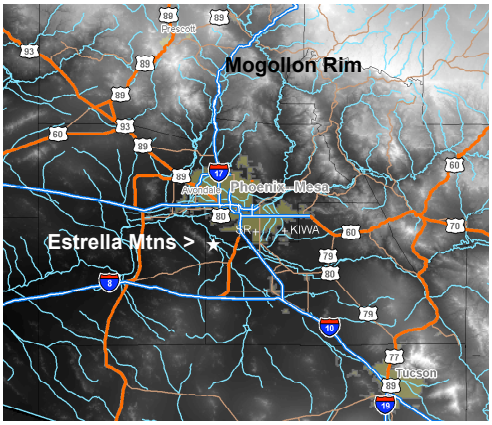


Figure 4. Grey shaded terrain image of Phoenix, Arizona and surrounding area. The southeast end of the Estrella Mountains is indicated by the star. SR1 and KIWA locations are shown to the southeast of the Phoenix metropolitan area.

(2001) described significant differences between tornado observations as sampled by different resolution volumes. Table 1 lists the resolution and scanning patterns for the SR1 and the KIWA WSR-88D. The range gate resolution for the WSR-88D is 1 km for reflectivity and 250 m for Doppler velocity. KIWA operated in volume coverage pattern (VCP) 11 that includes 14 constant elevation angle sweeps from 0.5 deg through 19.5 deg. The SR1 has a considerably finer range gate resolution of 70 m for both reflectivity and velocity. The SR1 azimuthal resolution is nearly identical to the WSR-88D. The SR1 VCP is variable and contains several more elevation sweeps, especially at lower altitudes. The KIWA radar completed a VCP in 5 min while the SR1 VCPs varied between 3 and 5 min.

Figure 4 shows a shaded relief image of central Arizona terrain and location of the radars on 27-28 July 2004. The Mogollon Rim to the north of PHX is a favored area for storm initiation, especially during the summer (Maddox 1995). During the afternoon of 27 July, a line of storms formed along the Rim with an associated outflow boundary moving toward Phoenix.

Since the SR1 radar was scanning the approaching gust front to the north, the downburst storm's formation is documented using data from the KIWA radar. The first cells developed at the SW end of the Estrellas around 0100 UTC. Storms in the western United States typically form along mountains that serve as an elevated heat source (e.g., Wakimoto 1985). It is hypothesized that the CI present in the sounding discussed in the previous section was overcome by terrain forcing. The northwestern-most cell in the short line was growing rapidly while the other cells decayed as they moved to the east-southeast.

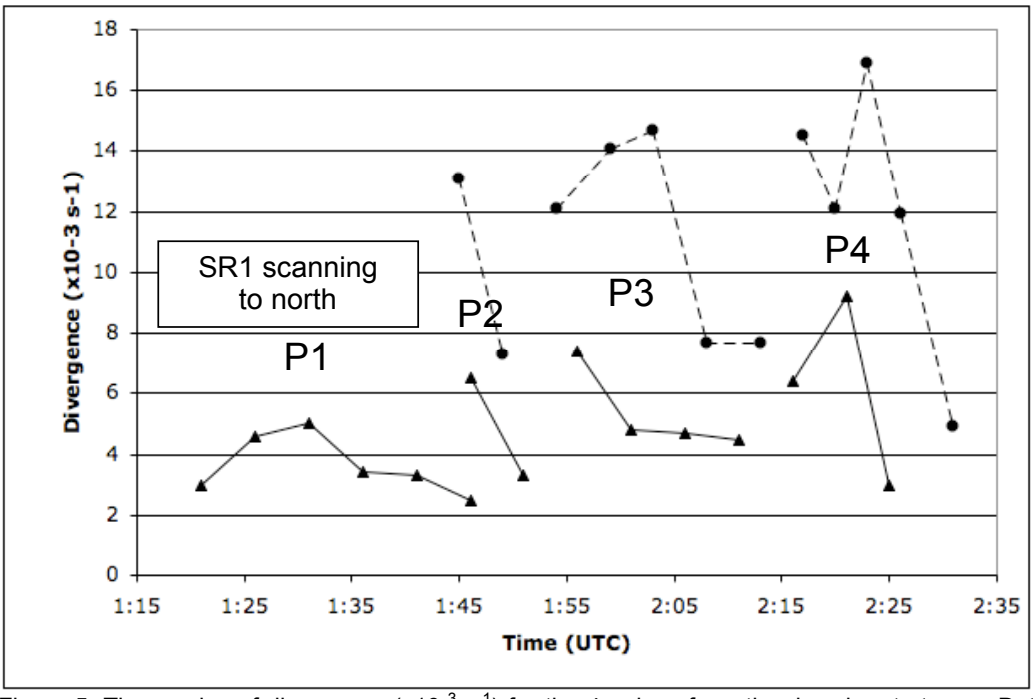


Figure 5. Time series of divergence ($x10^{-3}$ $s^{-1}$) for the 4 pulses from the downburst storm. Data are from the lowest elevation angle from each radar varying from 0.8 km to 0.7 km AGL for KIWA and ~0.6 km for SR1. The solid line is for KIWA and the dashed line is for SR1. Note that the SR1 was scanning to the north prior to 014400 UTC.

At 0119 UTC the storm top was near 9 km AGL with a divergent Doppler radial velocity difference ($\Delta v$) of 20 m $s^{-1}$. High reflectivity reached the surface and was accompanied the first downburst pulse P1 just before 0131 UTC with a divergence of 26 m $s^{-1}$ over a distance of 5.56 km (4.8 x $10^{-3}$ $s^{-1}$). While the dimensions were more pronounced with radial velocities 3-5 m $s^{-1}$ stronger. The rotational features were likely the result of the inferred downdraft as noted by Rinehart et al. (1995). Near storm top, both radars depicted small areas of divergence on the western edge of the cell complex, indicating new cell growth. The divergent radial velocities were stronger in the

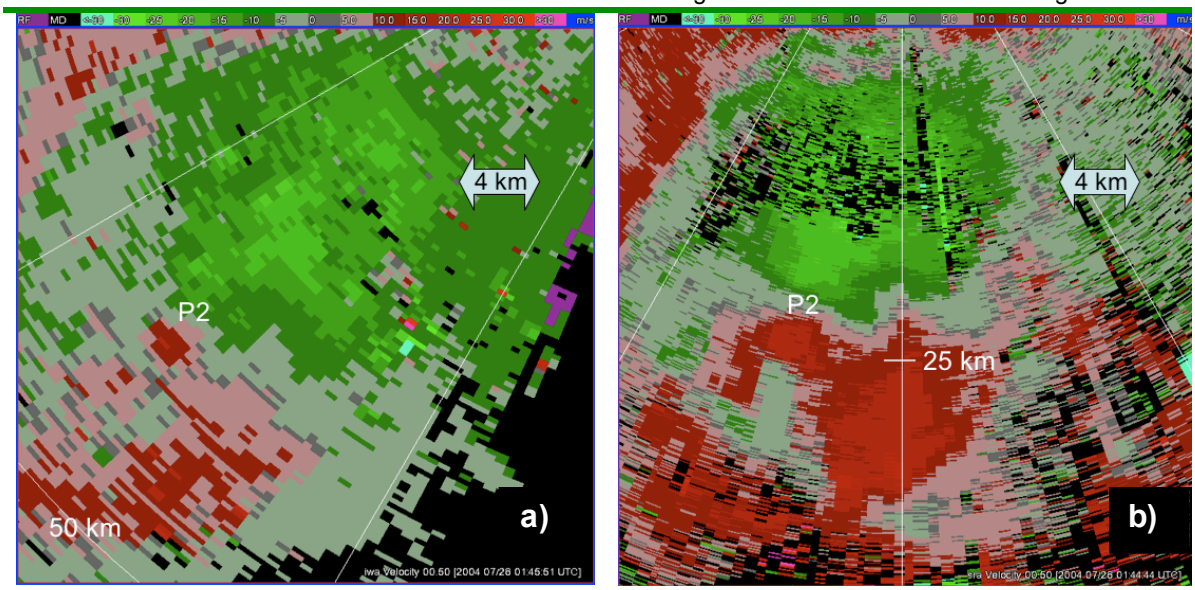


Figure 6. Radar images at 0.5 deg elevation of velocity for a) KIWA at 014551 UTC and b) SR1 at 014444 UTC.

of the outflows in this event conform to downburst definitions, peak divergence values often occurred over a smaller radial distance less than 4 km.

The SR1 radar began scanning the microburst storm at 014444 UTC as P1 was weakening and P2 was starting. By this time, the storm had assumed a multi-cellular appearance that was well defined by the high resolution of the SR1. Figure 6 compares velocity from both radars at low altitudes. Both radars show a cluster of small cells at the southern edge of the ring-shaped outflow boundary from the initial downburst. While differences between the velocity fields can be significant due solely to asymmetry and different viewing angles (see e.g., Hjelmfelt 1988), the SR1 data has stronger gradients along the gust front to the north, now impinging on the downburst outflow, and finer scale structure in the downburst divergence signature. The $\Delta v$ in P2 at 014551 UTC, as seen by the KIWA radar, was 22 m $s^{-1}$ across a distance of 3.7 km (5.9 x $10^{-3}$ $s^{-1}$) while the SR1 radar at 104444 UTC depicted a $\Delta v$ of 31 m $s^{-1}$ across a distance of 2.5 km (12.4 x $10^{-3}$ $s^{-1}$). Similar differences between the KIWA and SR1 data were seen aloft. For instance, the KIWA radar showed very weak mid-level rotation (not shown) while rotation couplets in the SR1 data SR1 radar data.

The initial pulses dissipated rapidly as the complex moved eastward. A third pulse P3 began just minutes later around 015403 UTC in nearly the same location as P1. Over the next 15 min, the sequence of mid-level images from the SR1 7.8 deg tilts showed intensification of mid-level rotation and convergence as the surface outflow expanded.

P3 produced a 67 mph gust observed at the Maricopa COOP site sometime between 0155 and 0205 UTC; the peak inbound velocity at 020321 UTC from the SR1 was 28 m $s^{-1}$, ~1 km to the east of the COOP site. The maximum radial velocity from the KIWA radar near this time was –21.5 m $s^{-1}$ at 020044 UTC. The photo in figure 2 was taken near this time. Hjelmfelt (1988) pointed out that rotors along the leading edge of a microburst can result in a local enhancement of winds as well as very small-scale convergence/divergence couplets. The structure of the outflow winds at 020321 UTC supports the presence of one or more rotors in this event; there appeared to be at least 2 convergence/divergence couplets ahead of the main divergence center. There is only a hint of these features at the next 0.5 deg tilt at 020800 UTC while the maximum velocity measured at any time by the SR1 was 31.5 m $s^{-1}$ at this time, well away form the center of the pulses, further supporting the presence of a

rotor. There were a few gates with higher radial velocities but the data are very noisy are not used.

As P3 dissipated, the mid-level rotation and convergence continued to increase. At 021240 UTC a short-lived "mini-pulse" (MP) appeared beneath the convergence zone, possible indicating a cause and effect. There was also a brief rotation signature associated with the MP. As P3 continued to weaken the rotation tightened into a small vortex resembling a mesocyclone while the convergence began to dissipate. During P3, divergence values for KIWA never exceeded 7.4 x $10^{-3}$ $s^{-1}$ while SR1

Table 2. Microburst type, average velocity difference, average distance between peak velocities, and average time to reach peak divergence for the studies mentioned in the text. N/A indicates that the data were not available from the study.

| Region (# samples) Reference | Microburst type | Ave. delta-v (m $s^{-1}$) | Ave. distance (km) | Ave. time to maximum divergence |
|---|---|---|---|---|
| Colorado (99) Wilson et al. 1984 | LRM | 22 (median) | 3.1 | 5-10 min |
| Florida 1991 (84) Rinehart and Bohro, 1992 | HRM | 15.7 | N/A | N/A |
| Florida 1992 (908) Rinehart et al. 1995 | HRM | 16.2 | 2.4 | N/A |
| Oklahoma (3) Eilts and Doviak, 1987 | HRM | 25 | 6 | N/A |
| Utah (1) Milke and Carle, 1987 | LRM | 41 (anemometer) | 1.8 | N/A |
| PHX (3) | Hybrid | 36.6 | 2.3 | 3-10 min |

divergence values exceeded 12 x $10^{-3}$ $s^{-1}$ for three consecutive scans.

The final pulse of note was P4 and was associated with a large reflectivity core east of the location of the previous pulses and an initial divergence of 14.6 x $10^{-3}$ $s^{-1}$ at 021722 UTC. This pulse was also coincident with the rotation aloft that had shrunk in size but peaked in intensity at this time with a gate-to-gate velocity difference (at constant range) of 22 m $s^{-1}$. The next three 0.4 deg sweeps from the SR1 were only 3 min apart and document the rapid evolution of P4. At 022006 UTC the divergence was 12.6 x $10^{-3}$ $s^{-1}$ (34 m $s^{-1}$ over a distance of 2.73 km) and increased to 17.1 x $10^{-3}$ $s^{-1}$ at 022253 UTC. Thus it appears that this pulse reached maximum strength in under 6 min. Three minutes later, the outflow had begun to dissipate with another apparent rotor on the northern leading edge. Mid-level rotation and convergence continued to dissipate with this last pulse.

## 5. SUMMARY AND CONCLUSIONS

The outflow winds associated with the 27 July 2004 microburst storm exhibited a series of at least 4 distinct downburst pulses over a period of just over an hour. The initial pulse was the result of a descending reflectivity core that was apparently accelerated downward by melting ice and evaporating liquid. A series of subsequent outflow pulses coincided with rapid mid-level rotation and convergence that both appeared to be an aftereffect of the downbursts. The pulses exhibited a wide range of scales ranging from 5 km to just over 10 km for the maximum inbound and outbound winds. Shears were calculated over smaller distances in order to determine the maximum values. For the peak divergence for the three downburst pulses observed by the SR1, the average maximum velocity difference was 33.5 m $s^{-1}$ across an average distance of 2.3. As shown in table 2, the resulting divergence values are much stronger than those (on average) observed in different parts of the country.

Overall, the SR1 velocities were 3-5 m $s^{-1}$ stronger than those from KIWA. Due to its higher resolution, divergence values computed using the SR1 data were 2-3 times greater than values computed from the KIWA radar data. Furthermore, at times the SR1 scanned the lowest elevation at 3 min intervals and still did not fully resolve the evolution of the outflows. Reasons for the difference in values include resolution, viewing angle, and beam height. Since the velocity differences were small, it is believed that the ability of the SR1 to resolve smaller features was the largest contributor to the greater divergence values as compared to the lower-resolution KIWA radar.

It is believed that this paper is the first to document the structure and evolution of a Sonoran Desert down/microburst storm. Comparisons to Colorado low-reflectivity microbursts and high reflectivity microbursts in the SE U.S. support the conclusion that this event was unique in that it was a long-lasting event with characteristics of both HRMs and LRMs, perhaps earning the designation as a hybrid reflectivity microburst.

*Acknowledgements.* The SMART-R deployment and data collection were facilitated by Salt River Project. The authors wish to thank Chuck Dempsey and Charlie Ester of Salt River Project for their continued support and Doug Green of

the Phoenix Weather Forecast Office for his helpful review and insight into the environmental data. The authors also wish to thank James Walter for providing the sounding figures and surface data.

**REFERENCES**

Atkins, N.T. and R. M. Wakimoto, 1991: Wet microburst activity over the southeastern United States: Implications for forecasting. *Wea. Forecasting*, **6,** 470–482.

Biggerstaff, M. I., and coauthors, 2005: The Shared Mobile Atmospheric Research and Teaching Radar: A collaboration to enhance research and teaching. *Bull. Amer. Meteor. Soc.*, **86**, 1263–1274.

Brown, R.A., 1992: Initiation and evolution of updraft rotation within an incipient supercell thunderstorm. *J. Atmos. Sci.*, **49**, 1997–2031.

Caracena, F., M. and M. W. Maier, 1987: Analysis of a microburst in the FACE meteorological mesonetwork in southern Florida. *Mon. Wea. Rev.,* **115,** 969–985.

Eilts, M. D., 1987: Low altitude wind shear detection with Doppler radar. *J. App. Meteor.,* **26,** 96–106.

_____ and R. J. Doviak, 1987: Oklahoma downbursts and their asymmetry. *J. App. Meteor.,* **26,** 69–78.

Ellrod, G., J. P. Nelson, M. R. Witiw, L. Bottos, and W. P. Roeder, 2000: Experimental GOES sounder products for the assessment of downburst potential. *Wea. Forecasting*, **5,** 527–542.

Fujita, T. T., 1981: Tornadoes and downbursts in the context of generalized planetary scales. *J. Atmos. Sci.*, **38**, 1511–1534.

Hjelmfelt, M. R., 1988: Structure and life cycle of microburst outflows observed in Colorado. *J. Appl. Meteor.*, **27**, 900–927.

Maddox, R. A., D. M. McCollum, and K. W. Howard, 1995: Large-scale patterns associated with severe summertime thunderstorms over central Arizona. *Wea. Forecasting*, **10**, 763–778.

Mielke, K. B. and E. R. Carle, 1987: An early morning dry microburst in the Great Basin. *Wea. Forecasting*, **2,** 169–174.

Rinehart, R. E. and A. Borho, 1992: A comparison of the detectability of microbursts in Orlando, Florida, by two c-band Doppler radars. *J. App. Meteor.,* **32,** 476–489.

_____, _____, and C. Curtiss, 1995: Microburst rotation: Simulations and observations. *J. App. Meteor.,* **34,** 1267–1285.

Storm Prediction Center (SPC) Online Severe Weather Climatology for Radar Coverage Areas: 1980-2005. Available at http://www.spc.noaa.gov/climo/online/rda/index.html.

Vasiloff, S. V., 2001: Improving Tornado Warnings with the Federal Aviation Administration's Terminal Doppler Weather Radar. *Bull. Amer. Meteor. Soc.*, **82**, 861–874.

Wakimoto, R. M., 1985: Forecasting dry microburst activity over the High Plains. *Mon. Wea. Rev.*, **113**, 1131–1143.

Wilson, J. W., R. D. Roberts, C. Kessinger, and J. McCarthy, 1984: Microburst wind structure and evaluation of Doppler radar for airport wind shear detection. *J. Appl. Meteor.*, **23**, 898–915.